DOI: 10.13009/EUCASS2019-669

Experimental study of energetic ionic liquid decomposition

Levard Quentin[1], Pelletier Nicolas[2], Byrde Lorenzo[3], Corato Christophe[4], Anthoine Jérôme[5]
[1] ONERA/DMPE Université de Toulouse, F-31410 Mauzac, France
[1] quentin.levard@onera.fr
[2] nicolas.pelletier@onera.fr
[3] lorenzo.byrde@onera.fr
[4] christophe.corato@onera.fr
[5] jerome.anthoine@onera.fr
Corresponding author: quentin.levard@ensta-bretagne.org

Abstract

Spacecraft attitude and control chemical thrusters are mostly based on catalytic decomposition of anhydrous hydrazine. Because of its high toxicity and suspected carcinogenic effect, CNES proposed for replacement a new family of green monopropellants based on energetic ionic liquids. For a proper design of thruster combustion chamber, experiments on thermal ignition and regression rate were necessary. An experimental study of the combustion of two HPGM (High Performance Green Monopropellant) is presented in this paper. Two experimental setups were developed to study monopropellant combustion. The first experiment is focused on an isolated droplet in a controlled atmosphere. Tuning initial pressure around fresh propellant highlighted that there is a threshold pressure below which there is no combustion, but only thermal decomposition of monopropellant. No regression of the hanged droplet was noticeable because of intense distortion effects. However, capture and track of some of the fragmented droplets allowed measuring their radial regression. Unfortunately, the spatial and temporal resolutions were not sufficient to provide an accurate measurement. This motivated the transition to a second setup called “U-gutter combustion setup”, which was designed to drastically increase the combustion duration and then the resolution of the regression rate measurement. Fast camera imaging and a “Time-wires” technique using thermocouples were implemented to measure the flame front displacement. The gutter is placed into a pressurized vessel allowing controlling the ignition initial pressure. During combustion, pressure is monitored to estimate pressure influence on regression rate. First results highlighted a strong dependency of pressure on regression rate. The three methods have given similar order of magnitude, repeatability experiments are necessary to conclude on methods accuracy.

1. Introduction

The European regulation on chemicals (REACh) threatens the use of hydrazine because of its highly carcinogenic and toxic effects [1]. Even though space propulsion represents a small part of the hydrazine industry, green propulsion is a major spatial research subject. Hydrazine is used since 1960 as a monopropellant without major technical innovations. Its decomposition on a Shell405 catalytic bed achieves a specific impulse of 220 s with a very high reliability. The main concern with hydrazine thrusters, except toxicity, is the catalytic bed degradation caused by thermal cycling. Because hydrazine has good performance, the requirements are very demanding for new thrusters. Electric propulsion is one of the rivals of chemical propulsion for attitude and orbit control because of its high specific impulse (2000 s) but the very low thrust of all electric technologies (Hall, ion grid, electrospray, etc.) is a major issue for high force or torque demanding manoeuvers.

Some chemical thrusters have been developed to challenge hydrazine thrusters, for instance the NASA’s GPIM AF-M315E [2] using hydroxylammonium nitrate or the FOI’s FLP-106 thruster based on ammonium dinitramide. Both of these thrusters use catalytic propellants based on energetic ionic liquids and increase performance from 30 to 50 % compared to hydrazine. This performance increase becomes a problem for the catalytic bed that is even though altered. This led CNES to promote research on a new family of green monopropellants based on energetic salts. These HPGM (High Performance Green Monopropellant) demonstrate low toxicity and high performance in terms of density and theoretical specific impulse [3]. Following a period of deep thermo-chemical characterizations, the project is now focused on the study of propellant ignition and combustion behavior, our main objective being to achieve a thermal ignition so as to get rid of catalysts. One of the main objectives of the project is to characterize the

DOI: 10.13009/EUCASS2019-669

the decomposition of HPGM prototypes, and more particularly their burning rate in order to optimize a complete thruster design. This work presents an experimental approach to observe the decomposition of two HPGM prototypes using two distinct experimental setups.

2. Observation of an isolated droplet of monopropellant decomposition in a controlled atmosphere

It is reported in literature that monopropellants show a more or less strong pressure dependency on regression rate and ignition [4] [5]. It is thus mandatory to study the effect of surrounding pressure on combustion in order to achieve a optimized thruster design. This implies to carry out all our experiments in a closed reactor with a fine ambience control. It was decided to set the pressure range between 0 and 10 bar in order to catch the full working interval of an orbital thruster (i.e. from vacuum ignition to maximum chamber pressure).

2.1 Experimental setup

There are many experimental approaches to observe and measure regression rate of new liquid propellants and fuels [4] [5] [6] [7]. Because the tracking of droplets in a spray is made difficult by the huge number of generated droplets, the most proper way to measure the regression rate of a liquid is to observe an isolated droplet. Many systems already exist to maintain a suspended droplet, such as magnetic fields, crossed fibers or even weightlessness systems (ex. drop tower, parabolic flights, space station). In this study, combustion occurs in a premixed flame, without any influence of natural convection. This is why the technique of droplet hanged on crossed fibers was chosen, assuming there is no impact of wires on combustion mechanism [8] [9].

Suspension of the droplet and temperature measurement

In order to observe a radial regression of the droplet, we choose to drop a millimeter sized droplet on micrometric fibers. The use of fibers induces a thermal loss by conduction through the fibers. A study has been realized by Chauveaux *et al.* [9] on the maximum size of fibers that permits to neglect the heat flux through the fibers. This study highlights a maximum limit of 14 µm for kerosene combustion [8].

In the present study, we choose to start the experiments with 100 µm tungsten fibers for reliability during the combustion of the monopropellant. Thinner fibers are available if necessary to reduce the heat flux through the support. For numerical comparison and phenomenon understanding, it might be interesting to measure the droplet temperature during the combustion. The droplet temperature is get by a micro-thermocouple hanged inside the droplet. One of the crossed fibers is replaced by the thermocouple so that the thermocouple is continuously inside the droplet. The thermocouple used is a 50 µm type K thermocouple, which is a good compromise between reliability and reactivity. Fibers and thermocouple are fixed on M1.5 screws with an epoxy bounding (2216 B/A for its good thermal strength). Before the fibers positioning, epoxy supports are placed on screws for electrical isolation purpose (Figure 1). To ensure the sealing of the thermocouple, a 1.5mm sleeved thermocouple is mounted with a sealed port and cut at its end to extract chromel and alumel wires. Finally, nude wires are welded to the micro thermocouple. The droplet is heated with a solenoid coil surrounding the crossed fibres. The solenoid is made with a 1 mm thick chromel wire due to its good oxidation resistance which allows multiple tests before the wire breaks. Solenoid steps are not constant for an easier visualisation of the droplet.

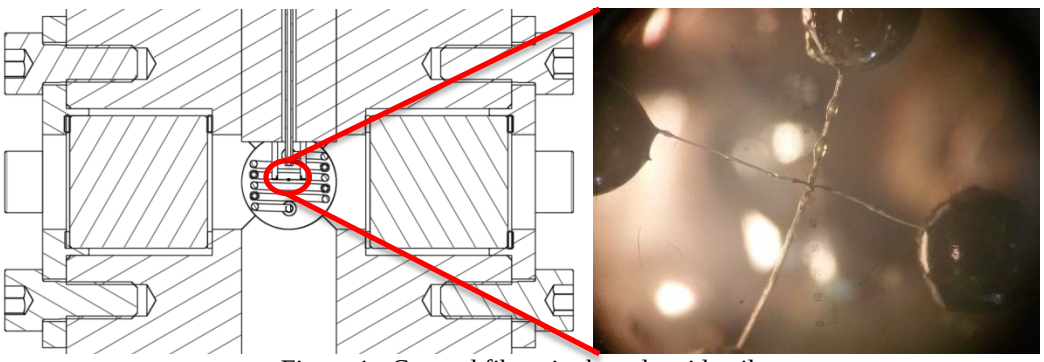

Figure 1 : Crossed fibres in the solenoid coil

DOI: 10.13009/EUCASS2019-669

Optical system for droplet observation

The initial objective of this device was to observe the radial regression of a hanged droplet. For radius measurement, it is possible to observe edges of the droplet using shadowgraphy. To do so, it is necessary to ensure that the illumination of the observed object (droplet) is greater than the luminous phenomenon (flame). Two light sources have been used and compared: a 1200W metal halide lamp and a 400W led with a matted filter. The latter has been retained for the sake of durability. Initial diameter of the suspended droplet is about 1 mm and 200 pixels on the diameter is thought enough to get a good resolution of the droplet, so the minimum size of pixels for radius measurement is 5x5 µm pixels. A V711 Phantom camera is used for its high speed and low shutter (2 µs) capabilities. The V711 sensor uses 20x20 µm pixels so a x4 magnification is necessary. A K2 Distamax long-distance microscope is used with a CF-2 lens, permitting a x2 magnification. The addition of a focal-doubler allows to reach a 5x5 µm pixel with the V711 sensor. In order to have a maximum field depth, the diaphragm is set as closed as possible to get equilibrium between shutter opening, frame rate, and brightness of the background. A short field depth permits a high precision on objects edges whereas a large field depth reduces the size dependency in the field depth (Figure 2).

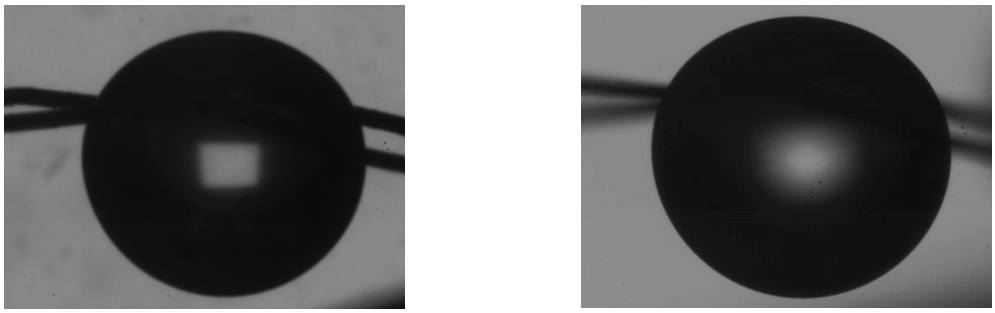

Figure 2 : Large field depth (left) versus short field depth (right)

Controlled atmosphere reactor

Like solid propellants, liquid monopropellants have highlighted pressure dependency on regression rate and ignition. In order to study the pressure impact on the monopropellant decomposition, a closed reactor provided by CNES is used (Figure 3).

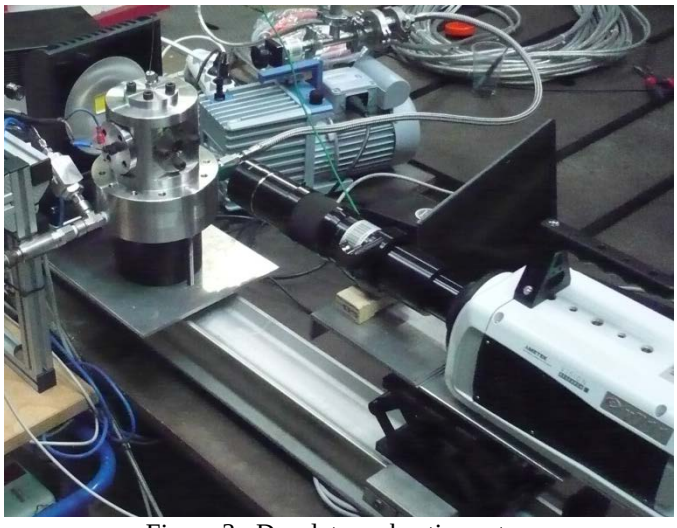

Figure 3 : Droplet combustion setup

This reactor is equipped with two quartz windows permitting shadowgraphy. Pressure range was set between 5.10^{-4} bar (primary vacuum) and about 10 bar in order to study both vacuum ignition phase and stationary combustion. For high pressure conditions, a N_2 tank with manual regulator is used to feed the reactor. For vacuum conditions, a vacuum pump (Vacuubrand RZ6) is also plugged. Vacuum and pressurization lines can be switched on demand without any dismounting/reassembly. For pressure measurement, a strain gauge sensor (General Electrics unik5000) is used for pressure over 1bar and vacuum sensor (Baratron capacitance manometer) for 0-1 bar pressure. The atmospheric valve is used to return to the atmospheric pressure after the experiment is completed (Figure 4).

DOI: 10.13009/EUCASS2019-669

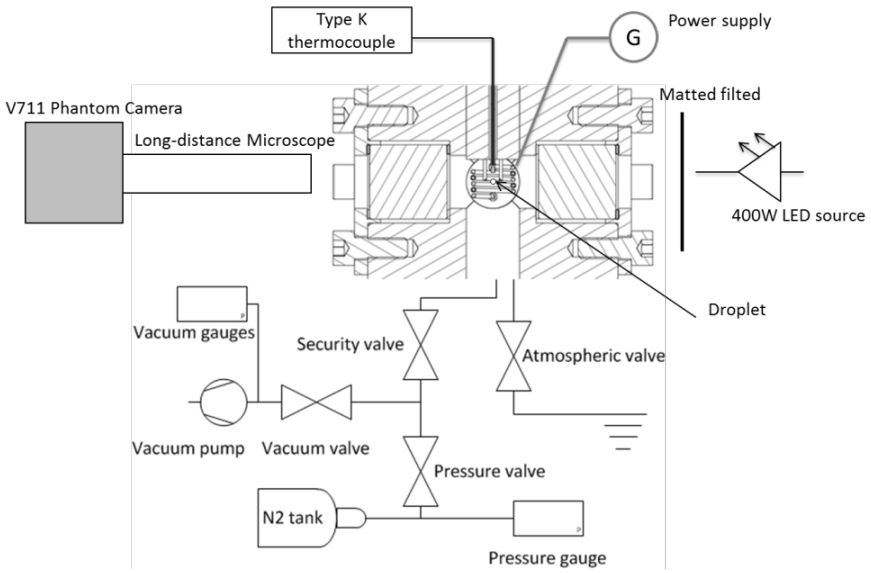

Figure 4 : Schematic of the experimental setup of droplet combustion

2.2 Image processing and droplet detection

First high speed image analysis revealed that the main suspended droplet get strongly distorted when its temperature get closer to the decomposition temperature, around 150°C. As a result, it is impossible to measure an equivalent radius of the suspended droplet. Two different regimes can nevertheless be distinguished: decomposition and combustion, separated by a threshold ignition pressure. Indeed, before this threshold, the droplet explodes and fragments in lots of finer droplets, but never regresses. On the contrary, over the threshold pressure, very few fragmentation is noticed, but regression appears on little droplets. One bar pressure steps were realized to find the rough ignition limit, which is around 5 bar.

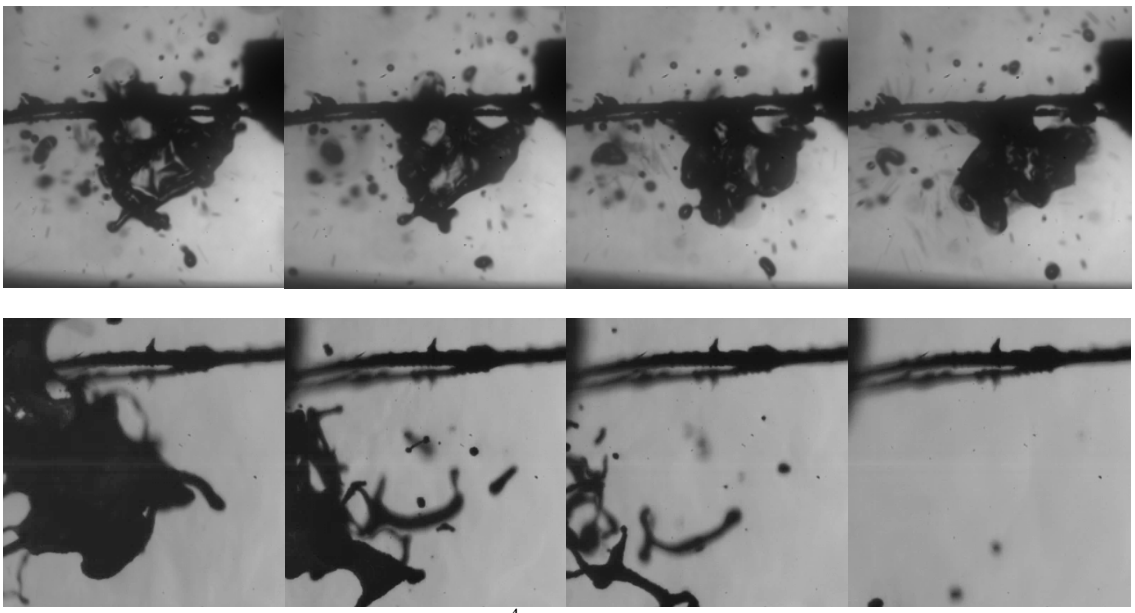

Figure 5 : Droplet decomposition at 5.10^{-4} bar (top); Droplet combustion at 11.5 bar (bottom)

DOI: 10.13009/EUCASS2019-669

Droplet detection

Since a regression has been observed, the regression rate of the liquid can be measured and the pressure dependency studied. The suspended droplet is too distorted during combustion to be analyzed. However, the little fragmented droplets are spherical because of their high surface tension, allowing their radius to be measured.

For blob detection, the “Maximally Stable Extremal Region” filter (MSER) has been highlighted as the most relevant detection method [10]. The MSER method is divided into three principal steps: in a first time a detection of local maximum intensity is realized over the image. Then intensity function is defined from the local maxima in all directions and threshold levels are covered to find stable regions. If the variation of area between two thresholding iterations is greater than the stability parameter, the region is excluded. Detected regions can also be selected by minimum and maximum area, or by diversity. Finally objects are approached with ellipses, extracting the center and the two ellipsis’s radius.

On native images, the MSER filter detects mostly the salt-and-pepper noise. The use of a 6x6 median filter could be used to remove salt-and-pepper noise but we observed that a high degree median filter reduces the apparent area of detected droplets. Finally, the subtractions of the background allow suppressing parasite dust on lens and drastically reducing the salt-and-pepper noise. After the background suppression, only a 2x2 median filter is necessary to totally remove salt-and-pepper noise without reducing the area of the detected objects (Figure 6).

Figure 6 : Native frame (left), post-processed frame (right)

Droplet tracking for regression measurement

The final objective is a regression measurement on fragmented little droplets. After detecting a cloud of droplets, it is necessary to track them over time to measure their radius variation. To this end, a tracking algorithm is implemented using a Kalman filter. The Kalman filter was proposed in 1960 by R. E. Kalman for noisy data treatment [11].

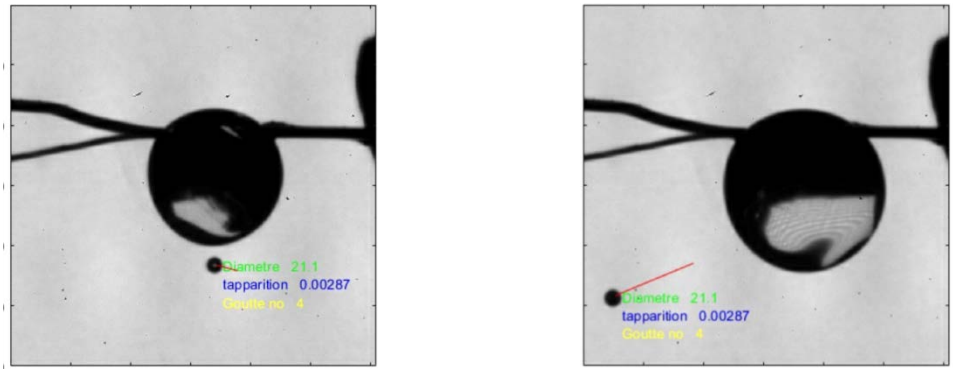

Figure 7 : Tracking of a droplet with a parabolic trajectory

For multiple-objects tracking, the algorithm is based on three principal steps. The first step is the detection of objects in a frame. Then, a prediction step is realized to predict the location of the detected objects position on the next frame. And finally, the association step to associate the predicted location with the detected objects of the next frame. In our case, the detection is realized with the MSER filter. The prediction of new state variable is done assuming a motion model (constant velocity or constant acceleration) considering processing noise and measurement noise.

DOI: 10.13009/EUCASS2019-669

Finally this prediction is compared to next objects detected through a cost function. This cost function can be defined as a comparison of distances, shape, size etc. Each detected object is therefore assigned to a track minimizing the cost. Tracks can be deleted if objects disappear and created if new objects are detected. In our case a constant acceleration model is considered with a large initial velocity error because droplet can be fragmented in all directions. In this configuration, most of considered droplets are tracked except rebounding droplets on the suspended one because of the acceleration variation due to impact. The Figure 7 presents the tracking of a droplet with a parabolic trajectory.

2.3 Results

Droplets of interest are selected in tracks results. Their regression rate is estimated with a linear regression of their radius. Figure 7 presents the results of the regression rate measurement for 7, 9 and 11.5 bar. We observe that even if the three inconsistent points (over 0.5m/s) are removed, the standard deviations are respectively 0.064, 0.040 and 0.018. This deviation can be the result both droplet observation and radius measurement. Even if the field depth is as large as enabled by the backlight, some droplets become blurred when they move away from the focal plane. Moreover, the experiment was originally designed to observe the regression of the main suspended droplet. As a consequence, spatial resolution becomes insufficient to provide an accurate measurement of 20 µm droplets and less. Finally it is not possible to measure precisely the regression rate with this setup but. There is indeed no clear tendency as regards pressure effect on regression rate, the latter appearing to be more or less constant, even decreasing, in the studied pressure range.

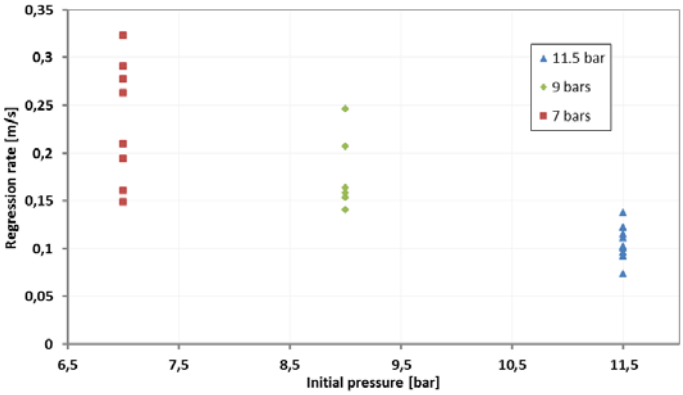

Figure 8 : Regression rates of droplet at 7, 9 and 11.5 bar

3. Regression rate measurement in a U-gutter

Strand burners are widely used for regression rate measurement for solid propellant and monopropellants. For solid propellants, strand burners (or Crawford burners) names a vertical propellant sample, ignited at it extremity, and inhibited on the others surfaces [12]. For liquid monopropellant study, samples are filled into vertical transparent chamber [4] [5]. In most study, propellants are ignited with hot wires and placed into a closed vessel to study the pressure dependency on regression rate. In this study, the liquid is placed in a U-gutter to reduce the auto-compression effects of the flame front that can appear in a vertical tube.

3.1 Experimental setup

A dedicated flame velocity test bench has been designed for the specific case of premixed liquid monopropellants. The main part of the bench is a close vessel equipped with fluidic, electric and measurement ports (Figure 9). The vessel was designed to withstand a maximal pressure of 80 bar. Vessel pressurization is achieved by a N_2 circuit controlled by a pressure strain gauge sensor (General Electrics unik5000). A 6x6x200mm U-gutter is inserted in the vessel and can contain a maximal volume of propellant of about 7 mL. An original improvement is that the gutter is thermalized thanks to an internal heat-transfer fluid loop linked to a thermocryostat (Lauda ProLine RP 1845C). This allows a precise control of the propellant temperature before ignition in the range 0-40°C, and, *in fine*, the study of the effect of fresh propellant temperature on regression rate. Upper side of the vessel receives a rectangular quartz porthole allowing a full observation field of the gutter.

Two complementary methods of regression rate measurement are used. First, non-intrusive high velocity imaging (Phantom V711) is used to follow the flame front. Imaging is realized either in the visible range or in the far infrared in order to reduce sensor illumination. Secondly, a classical “Time wires” intrusive technique as been adapted. Its

DOI: 10.13009/EUCASS2019-669

rather simple principle consists in measuring the time between two adjacent gates placed all the gutter along. Gates can be fuse wires or even thermocouples. The latter are preferred because we can get additional thermal information. Up to 20 type K thermocouple gates can be placed on the gutter, leading to a spatial resolution of 10 mm. A tailor-made high pressure lead-through has been conceived for the routing of the wiring from the gutter to the DAQ.

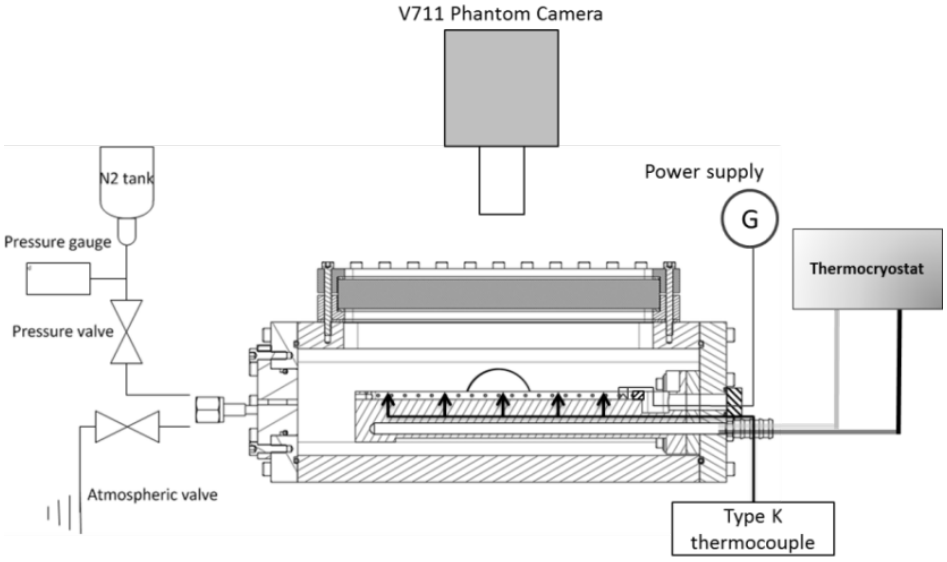

Figure 9: Schematic of pressurized U-gutter setup

3.2 Flame detection and data processing

Preliminary experiments were realized in order to observe the ignition in the gutter. The gutter length was reduced to 7 cm and observed in the visible domain with a standard color camera Casio EX-F1 at 25 µs shutter and a V711 at 1 µs shutter. We can see on Figure 10 a dazzle due to a too large exposure time for both visible view (top and middle). In order to protect the sensor of the V711 camera, an IR filter (>800 nm) has been added (Figure 9, bottom).

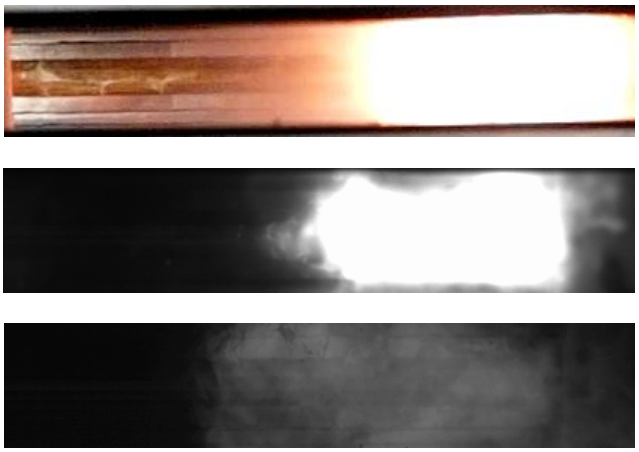

Figure 10: View of the flame front with a fast imaging in the visible domain colour (top), fast B/W camera (middle), infrared (bottom)

Thermocouple detection

Figure 11 presents the temperature and pressure measurement for a 20 cm gutter combustion equipped with 6 thermocouples. These thermocouples named Tcx from 1 to 6 respectively are placed at 5 10 14 16 18 and 20cm from the ignition edge. We can see that all temperature signals have the same profile and are in good agreement with their position in the gutter.

In order to calculate the regression rate of the liquid, it is necessary to detect when each probe emerge from the liquid. The time taken by each thermocouple to cross the liquid front is determined by the intersection between the

DOI: 10.13009/EUCASS2019-669

asymptotic initial temperature and the tangent line to the maximal derivate (which is located at the inflection point of the temperature curve). Crossed with the positions of thermocouples, it is possible to measure the successive positions of the liquid front. A ϵ coefficient is used to correct the time onset in order to match the pressure pick reached at combustion end with the last thermocouple signal.

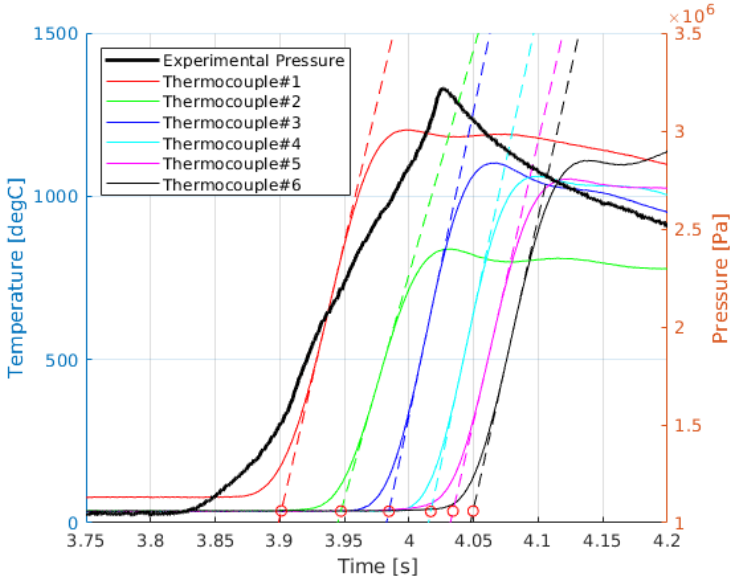

Figure 11 : Experimental pressure and temperature curves showing tangent at the inflection point (dashed lines) and temperature rise onset (red circles)

Image processing

Two different imaging approaches have been retained to follow the flame front during combustion. The first approach is the measurement of the maximum intensity position and the second approach is the measurement of the barycenter position of a box surrounding the flame (cf. Figure 12). All the image processing is made with ImageJ [13].

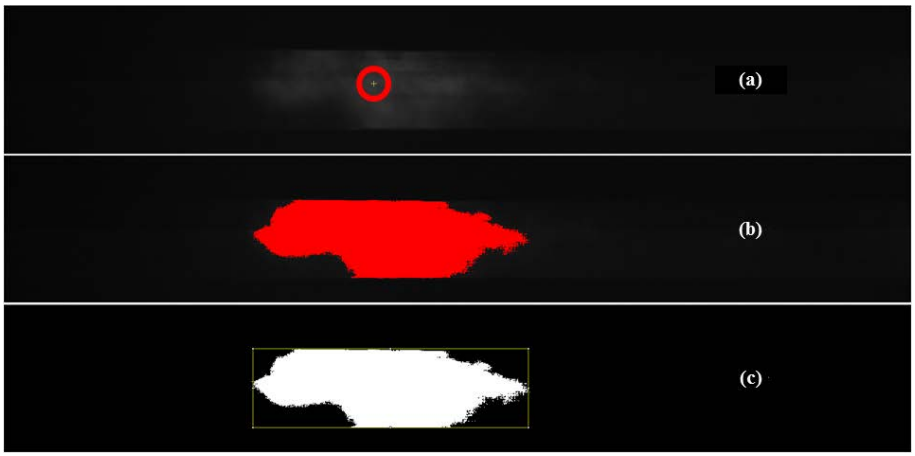

Figure 12: (a): Raw image with local intensity maximum (yellow dot in red circle); (b): Otsu dynamic threshold; (c): bounding rectangle of the newly obtained particle.

Following the image processing, we obtain tables listing the position of the intensity maxima and the characteristics of the bounding rectangles. These outputs can be used along with the pressure readings for the second and final part of our data processing: the calculation of the regression speed as a function of pressure via Matlab[1].

[1] Source: MATLAB. (2019). version 9.5.0 (R2018b). Natick, Massachusetts: The MathWorks Inc.

DOI: 10.13009/EUCASS2019-669

Burning rate calculus

The first objective of this data processing section is to read, filter and smooth the data acquired by ImageJ. As there can be more than one local intensity maximum and/or bounding rectangle per image, it is necessary to ensure that every outlier is removed before proceeding onwards. This is done by using the *isoutlier* function[2] on the x position of the intensity maxima and on the area of the bounding rectangle. This function labels as an outlier any element more than three local scaled Median Absolute Deviations from the local median over a window length specified by the user. These outliers are then removed from the data in order to proceed to the data smoothing; Smoothing then performed on the remaining points via the use of the *smoothdata* function[3] which returns a moving average of the data using a window length specified, once again, by the user. The comparison of the raw and clean data for both methods ("maximum intensity method" and "bounding rectangle method") can be seen in Figure 13. Please note that the origin of the positions shown is arbitrary which corresponds, in our case, to the lowest position of the curve – hence explaining the offset that can be seen between the Raw and Smooth positions for each method.

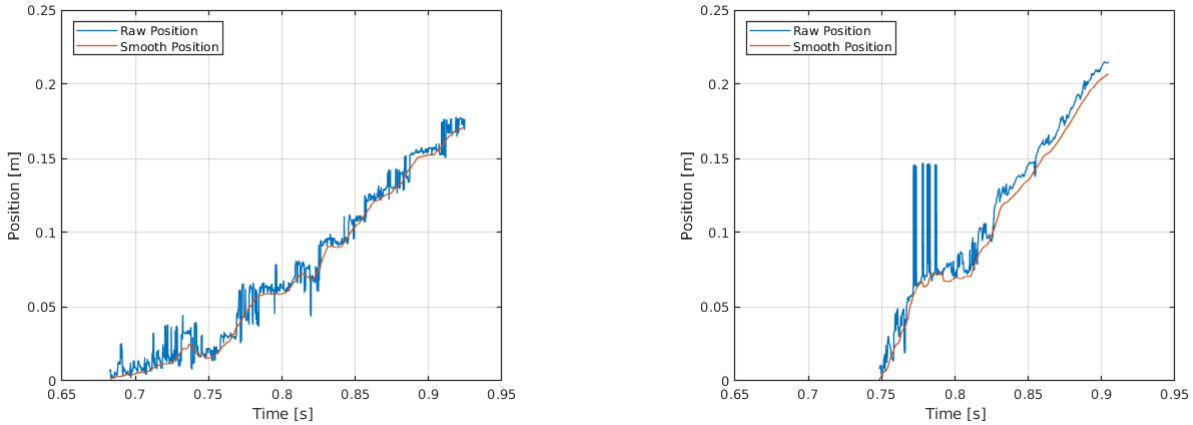

Figure 13 : Comparison of raw and clean positions for both methods: (left) maximum intensity method ; (right) bounding rectangle method

These values of position can then be used to fit a curve (exponential or polynomial in our case) which will then be derived to obtain the velocity of regression through time. As the pressure according to time is already known (cf. Figure 11), it is therefore possible to reach a value of regression rate as a function of pressure as seen in the Figure 14 of section 3.3 Results.

3.3 Results

The results presented in this section are preliminary results prefiguring a complete test campaign. The Figure 13 shows regression rates as a function of pressure with both optical and thermocouple methods. Both results appear to be rather linear on this pressure range. We can observe the same inflection point around 18 bar, which is not understood to date. In order to have a validation of the measured burning rates, this data are integrated over time, giving the total distance covered by the flame.
It appears that the bounding rectangle and thermocouples methods both return similar burning rates. Regarding the maxima method, its lower burning rate could come from the structure of the flame itself. Indeed, as, in our case, the brightest UV area of the flame is behind the centre of the bounding rectangle and as the flame significantly grows during the test, the speed at which evolves the intensity maximum is therefore lower than the centre of the bounding rectangle (and thus than the thermocouples method).

[2] Source: https://fr.mathworks.com/help/matlab/ref/isoutlier.html
[3] Source: https://fr.mathworks.com/help/matlab/ref/smoothdata.html

DOI: 10.13009/EUCASS2019-669

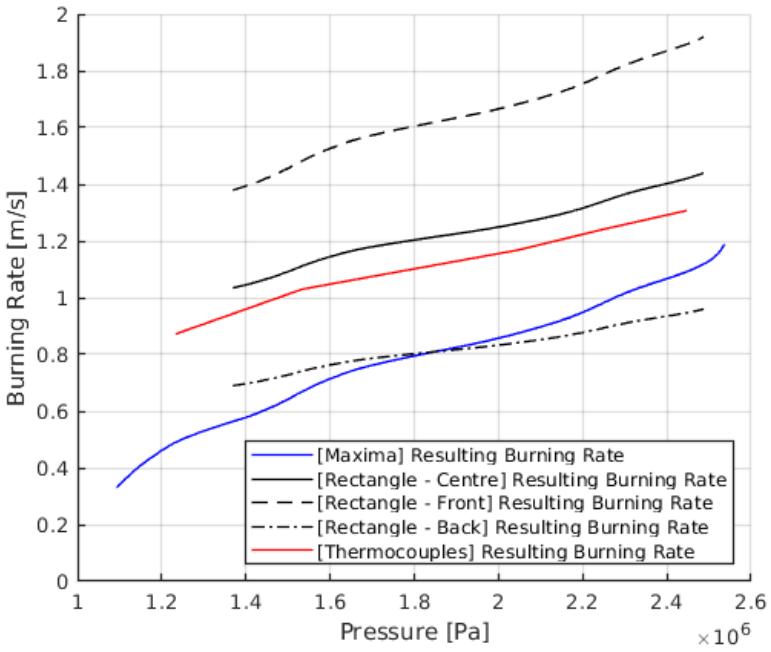

Figure 14 : Regression rate as a function of pressure: Thermocouples method, image processing with “bounding rectangle method” (centre, front and back) and “maximum intensity method”

This process returned a total travel distance of 21.6 cm for the “maximum intensity method” and of 34.9 cm for the “bounding rectangles method”. As the total length of the U-gutter is equal to 20 cm (cf. section 3.1 Experimental setup), the “maximum intensity method” appears to be more adapted to our experiment. The integrated distance of the thermocouple method is 23.6 cm, pointing out a correct agreement with the gutter length.

4. Conclusion and perspectives

In order to measure the regression rate of new energetic ionic liquids, two experimental setups were developed. In a first time, experiments were carried out on isolated droplet in a controlled atmosphere, ignited with a surrounding coil. These experiments highlighted two different regimes separated by a threshold pressure around 5 bar. The first regime is characterized by a strong fragmentation of droplets, but no regression. The droplet seems to decompose under the coil heating. Over the threshold pressure, we observe less fragmentation but a regression is visible. Detecting and tracking regressing droplets permitted first measurement of regression rate but temporal and spatial resolutions were not sufficient to conclude on pressure influence.

In order to increase accuracy, a 20 cm long U-gutter has been used for combustion measurement. For position measurement, two methods were implemented to detect the liquid front: 6 thermocouples used as physical gates and fast imaging. These two methods results are similar but cannot be compared on the same experiment for now due to thermocouple luminosity when burned. A possible solution to overcome this issue might be to hide the thermocouple wires from the camera. Finally, the regression rate was calculated as a function of pressure with the three methods and give similar results in the pressure range of the study. Integration of the calculated regression rate stated that the “bounding rectangle method” overestimates the regression rate, nevertheless the “maximum intensity method” and thermocouple method integration point out a good agreement with the gutter length. Reproducibility has been verified with this experiment and the same monopropellant.

Finally, it would be interesting to start the ignition of the liquid at a lower surrounding pressure in order to compare results with the isolated droplet regression rate. During experiments, a dependency of ignition on the initial thermal control of the gutter was noticed and should be explored to get a two-dimensional mapping of the burning rate $v_b(P,T)$.

DOI: 10.13009/EUCASS2019-669

Acknowledgement

This research was conducted in the framework of a joint project funded by CNES and ONERA on green monopropellant research. Authors would like to thank Duc Minh Le, Jean-Yves Lestrade, Jouke Jan Hÿlkema and Patrick Jezequel for their help during experimental setups preparation and propellant formulation.

References

[1] S. Tissot and A. Pichard, “Seuils de toxicité aiguë hydrazine (NH2NH2) - INERIS-DRC-02-25590-ETSC- STi - ,” Ministère de l'écologie et du développement durable ministère de la santé, de la famille et des personnes handicapées, 2003.

[2] R. A. Spores, R. Masse and S. Kimbrell, “GPIM AF-M315E Propulsion system,” *49th AIAA/ASME/SAE/ASEE Joint Propulsion Conference &Exhibit*, 2013.

[3] N. Pelletier and J.-Y. Lestrade, “Overview of the CNES “High Performance Green Monopropellant Project”: Requirements, Organization & Breakthroughs,” in *Space Propulsion*, Sevilla, Spain, 2018.

[4] Y. Ide, T. Takahashi, K. Iwai, K. Nozoe, H. Habu and S. Tokudome, “Potential of ADN-based ionic liquid propellant for spacecraft propulsion,” in *2014 Asia-Pacific international symposium on aerospace Technology*, 2014.

[5] S. Wang and S. T. Thynell, “Decomposition and combustion of ionic liquid coumpound synthesized from N,N,N',N'-tetramethylethylenediamine and nitric acid,” in *American Chemical Society*, Washington DC, 2012.

[6] L. Gupta, L. Jawale, M. Maurya and B. Bhattacharya, “Various methods for the determination of the burning rates of solid propellants - an overview,” *Central European Journal of Energetic Materials* , vol. 3, no. 12, pp. 593-620, 2015.

[7] Y.-Z. Pan, Y.-G. Yu, Y.-H. Zhou and X. Lu, “Measurement and analysis of the burning rate of HAN-based liquid propellants,” *Propellants, Explosives; Pyrotechnics*, vol. 37, pp. 439-444, 2012.

[8] Y. C. Liu, C. T. Avedisian, K. N. Trenou, J. K. Rah and M. C. Hicks, “Experimental study of initial diameter effects on convection-free droplet combustion in the standard atmosphere for n-heptane, n-octane, and n-decane : international space station and ground-based experiment.,” *American institute of aeronautics and astronautics*, vol. 52, 2014.

[9] C. Chauveau, F. Halter, A. Lalonde and I. Gökalp, “An experimental study on the droplet vaporization : effects of heat conduction through the support fiber.,” Como Lake, 2008.

[10] K. Mikolajczyk, T. Tuytelaars, C. Schmid, A. Zisserman, J. Matas, F. Schaffalitzky, T. Kadir and L. Van Gool, “A comparison of affine redion detectors,” in *International Journal of Computer Vision*, 2005.

[11] R. E. Kalman, “A new approach to linear filtering and prediction problems,” in *Journal of basic engineering*, 1959.

[12] N. Kobuta, Propellants and explosives, thermochemical aspects of combustion, 2002.

[13] C. A. Schneider, W. S. Rasband and K. W. Eliceiri, NIH image to ImageJ : 25 years of image analysis, vol. 9 (7), Nature methods, 2012, pp. 671-675.